Forest Ecology and Management 567 (2024) 122067

Contents lists available at ScienceDirect

Forest Ecology and Management

journal homepage: www.elsevier.com/locate/foreco

Assessing the impact of Hurricane Ivan on aboveground forest carbon dynamics in the Florida Panhandle: A case study from Perdido Bay watershed

Asiful Alam [a,b,*], Parag Kadam [b], Thomas Brandeis [c], Andres Baeza-Castro [c], Puneet Dwivedi [b]

[a] *Department of Forest Engineering, Resources and Management, Oregon State University, Corvallis, OR 97331, United States*
[b] *Warnell School of Forestry and Natural Resources, University of Georgia, Athens, GA 30602, United States*
[c] *Southern Research Station, Forest Inventory & Analysis, US Forest Service, Knoxville, TN 37919, United States*

ARTICLE INFO

Keywords:
Carbon dynamics
Forest inventory analysis
Hurricanes
Log-linear regression
Vulnerability

ABSTRACT

Hurricanes can physically transform forest ecosystems, leading to immediate and potentially long-lasting impacts on carbon dynamics. Using Forest Inventory Analysis (FIA) data from the United States Forest Service, we compared the average carbon in trees (saplings, bole, stump, tops) and foliage pre- (2001–2003) and post- (2005–2007) Hurricane Ivan for different tree categories in the Perdido Bay Watershed located in the Florida Panhandle. The log-linear regression model indicates that variables stand type (softwood/mixed/hardwood), diameter, height, physiographic class (deep sands/flatwoods/rolling uplands/small drains/swamps/bottomlands), elevation, field age and plot affected status were statistically significant ($p \leq 0.05$) determinants of carbon loss from the forest stands. Results showed that plots with medium-diameter stands lost more aboveground carbon than large and small-diameter stands, similarly, softwood-dominated stands lost more aboveground carbon than hardwood and mixed wood stands. Aboveground carbon decreased in stands with large (≥ 0.15 m) and medium (≥ 0.12 m) diameter-at-breast height (DBH) by 22.74 and 30.22 metric tons/ha, respectively. We ascertained a decrease of 74.51 and 17.82 metric tons/ha of aboveground carbon in hardwood and mixed plots after Hurricane Ivan, respectively. Aboveground carbon in young (< 25 y) taller trees (> 15 m) decreased by 121.55 metric tons/ha of carbon immediately after the hurricane. These findings underscore the critical necessity of comprehending the interplay between forest structure and hurricane activity to forecast the repercussions of such disturbances on carbon stocks. Our provided framework serves as a valuable tool for researchers and policymakers to assess the vulnerability of coastal forests and facilitate strategic planning to protect forests as carbon sinks.

1. Introduction

The Intergovernmental Panel on Climate Change (IPCC) climate change 2023 synthesis report AR6 states that human activities are the primary cause of global warming, leading to an increase in global surface temperature of 1.1°C above the pre-industrial period (1850–1900) over 2011–2020 (IPCC, 2023). Human-induced climate change impacts numerous extreme weather events and climate patterns worldwide (IPCC, 2015), resulting in widespread adverse impacts on the environment and human populations (Kemp et al. 2022; Jehn et al. 2022).

Due to global warming, tropical storms and hurricane activities in the Atlantic Ocean, the Caribbean, and the United States (US) Gulf of Mexico have increased since 2000 (Stewart, 2011). About 6–7 hurricanes have formed in the North Atlantic every year since 1878, and roughly 2 per year land on the US coast (Sweet et al., 2022; NOAA, 2021a). According to the total annual Accumulated Cyclone Energy Index, hurricane intensity has risen noticeably over the past 20 years, and eight of the ten most active years since 1950 have occurred since the mid-1990s (US EPA, 2022). This suggests at least the possibility of a large anthropogenic influence on hurricane activity in light of rising global surface temperature. The relationship between tropical Atlantic sea surface temperature and hurricane activity infers that future changes in Atlantic hurricane activity will be accompanied by substantial increases in hurricane destructive potential, i.e. roughly a 300 % increase

* Correspondence to: Department of Forest Engineering, Resources and Management, Oregon State University, 216 Peavy Forest Science Center, Corvallis, OR 97331, United States.
E-mail address: asifulas@oregonstate.edu (A. Alam).

https://doi.org/10.1016/j.foreco.2024.122067
Received 28 February 2024; Received in revised form 4 June 2024; Accepted 5 June 2024

in the Power Dissipation Index by 2100 (Vecchi et al. 2008).

Damage from tropical storms and hurricanes in the US and elsewhere around the Atlantic basin is expected to continue to double every generation because of increasing population and infrastructure along the US coast (IPCC, 2014; U.S. Global Change Research Program, 2018). Economic damage from hurricanes in the US has increased significantly since 1900, and the dominant driver of the increase has been the historical rise in the amount and economic value of built infrastructure and wealth along the coast (GFDL, 2023). Since 1980, 32 catastrophic hurricanes and tropical cyclones have hit the US Southeastern and Gulf Coasts. The approximate cost of damages from these tropical cyclones and hurricanes was $1.3 trillion (NOAA, 2021b; NCEI, 2022). The year 2017 was the costliest in terms of cumulative costs; 16 separate billion-dollar weather events cost $306.2 billion, breaking the previous cost record of $214.8 billion in 2005 (NCEI, 2022).

Hurricanes cause adverse impacts on forest structure and composition (Xi et al. 2008b; Zhang et al. 2016; Sharma et al. 2021) and have major influences on the recovery of the coastal forests (Murdiyarso et al. 2015). Zeng et al. (2009) estimated that an average of 147 million trees were affected each year between 1851 and 1900, and these damages contributed to 79 million metric tons of annual carbon loss. They inferred that more forests were impacted and greater biomass lost between 1851 and 1900 than during the 20th century; the average annual forest impact and biomass loss between 1900 and 2000 were 72 million trees and 39 million metric tons (Zeng et al. 2009). Chambers et al. (2007) developed a Monte-Carlo model to calculate stem density, biomass distribution, mortality, and damage for all forested pixels using Landsat (30 m) and MODIS (500 m) satellite imageries and estimated about 320 million large trees were severely damaged with a total carbon loss of 53 million metric tons by hurricane Katrine in 2005. Another study from Negrón-Juárez et al. (2010) quantified forest disturbance (downed, dead, and snapped trees) produced by hurricanes using a relationship between tree mortality and Landsat (30 m) data that can be broadly applied to Gulf Coast forest ecosystems impacted by Hurricane Katrina and Rita. The study showed about 43.9 ± 8.4 million metric tons and 37.9 ± 6.4 million metric tons of carbon loss due to Hurricanes Katrina and Rita in 2005, respectively. Their results provided an important contribution to reliable assessments of large-scale disturbance produced by hurricanes in forest ecosystems.

Quantification of forest carbon is usually associated with a high degree of uncertainty due to differing methods or incomplete assessment of carbon pools after a significant hurricane (Houghton et al. 2012; Peneva-Reed et al. 2021). Researchers are developing models to predict the probability of hurricanes and the amount of damage inflicted by them to support overall decision-making and mitigate these catastrophic effects on forests (Peltola et al. 1999; Blennow and Sallnäs, 2004; Schmidt et al. 2010). Some models are used for quantifying damage at the single tree level (Schmidt et al., 2010), while others are used for stand-level projections (Hanewinkel et al. 2014) or regional-level assessment (Talkkari et al. 2000). There is a scarcity of studies on aboveground carbon changes at the anatomical level, including sapling, bole, stump, top, and foliage. Attention is needed to monitor aboveground carbon at the overall tree level, impacting carbon sequestration, forest health, resilience, biodiversity, and ecosystem functioning. By monitoring carbon at the tree level, we can better understand how much carbon individual trees are sequestering through photosynthesis and storing in their biomass. This information helps quantify the overall carbon sequestration capacity of forests accurately. Monitoring carbon levels can help detect stress factors such as drought, nutrient deficiencies, or disease, which may affect tree growth and vitality. Early detection of such issues allows for timely intervention to mitigate their impacts and maintain overall forest health. Understanding carbon dynamics at the tree level can provide insights into a forest's resilience to environmental stressors such as climate change or disturbances like wildfires or insect outbreaks.

The goal of our study is to quantify the impact of Hurricane Ivan on carbon at the anatomical level of tree in the Perdido Bay watershed located in the Florida Panhandle. Our first objective is to compare aboveground carbon at the anatomical level of the trees located inside the Perdido Bay watershed between pre- (2001–2003) and post- (2005–2007) Ivan period. Secondly, we assess the changes of aboveground carbon in different anatomical levels of the trees after Hurricane Ivan and the relevance of different tree characteristics using a log-linear regression model. Our study on aboveground carbon across different anatomical levels provides valuable insights into forest health and resilience, especially after catastrophic hurricanes. This assessment also enhances our understanding of tree mortality and carbon loss patterns in coastal forests.

2. Methods and Mmethodology

2.1. Perdido Bay and Hurricane Ivan

Perdido Bay (Fig. 1) covers approximately 13,000 ha. Its watershed encompasses over 323,800 ha of land, tributaries, lagoons, and bayous in Florida and Alabama. Perdido Bay is oriented almost perpendicular to the Gulf of Mexico, with a length of 53 km and an average width of 4 km (Taylor et al. 2002). Perdido Bay is connected to the Gulf of Mexico through Perdido, and the Gulf Intracoastal Waterway (GIWW) passes through the southern portion of the bay, including areas along the coastal and inland sections of Escambia County in Florida and Baldwin and Escambia counties in Alabama.

Hurricane Ivan hit Perdido Bay on the morning of 16 September 2004 as a category 3 hurricane with sustained winds of 193 km/h and a 4.3 m storm surge, causing tremendous wind and water damage (National Weather Service 2005). Hurricane Ivan ravaged the coastlines of Mississippi, Alabama, and Florida, producing waves over 15 m high offshore. By the time it completely dissipated nearly a week later, Ivan had claimed the lives of 57 people and caused more than $27 billion of damage (in 2017 dollars) (National Weather Service 2005; Stewart, 2011).

2.2. Data collection and data processing

We obtained the Forest Inventory Analysis (FIA) database for Florida and Alabama from the publicly available FIA DataMart website (https://apps.fs.usda.gov/fia/datamart/datamart.html), then selected plot level data within our study area using ArcGIS Pro v2.8 software and processed these data following the steps illustrated in Fig. 2. We utilized the "RSQLite" and "sqldf" packages in R programming software v3.0.1 (R Core Team, 2021) to connect and manage the database. We extracted data from three annualized database tables, namely *PLOT, COND*, and *TREE*, over a period of 2001 and 2007. We focused only on accessible forestland for our study because those are part of the population of interest and safe to occupy, have at least 10 % canopy cover from live tally trees of any size, or have historically had at least 10 % canopy cover from live tally species inferred from the presence of stumps, snags, or other indicators (O'Connell et al., 2016). The filtered data for the selected seven years were exported to.csv files for further processing in ArcGIS Pro v2.8 and geolocation cross-validation with our study area (Supplementary Table T1). We shared our FIA plot locations with the USDA Forest Service Southern Research Station scientists to validate the geolocation for our study area. They applied the "fuzzing and swapping" technique to maintain, check, and validate the geolocation as per the privacy requirements specified in the Privacy Act of 1974 (Coulston and Reams, 2005; LaPoint, 2005). Then, we delineated our plot locations inside the Perdido Bay watershed with an assumed buffer zone of influence of 80 km along the track of Hurricane Ivan (Fig. 1).

Forest inventory plans are designed to meet sampling error standards for area, volume, growth, and removals provided in the Forest Service directive (FSH 4809.11), known as the Forest Survey Handbook (USDA, 2003). These standards, along with other guidelines, are aimed at

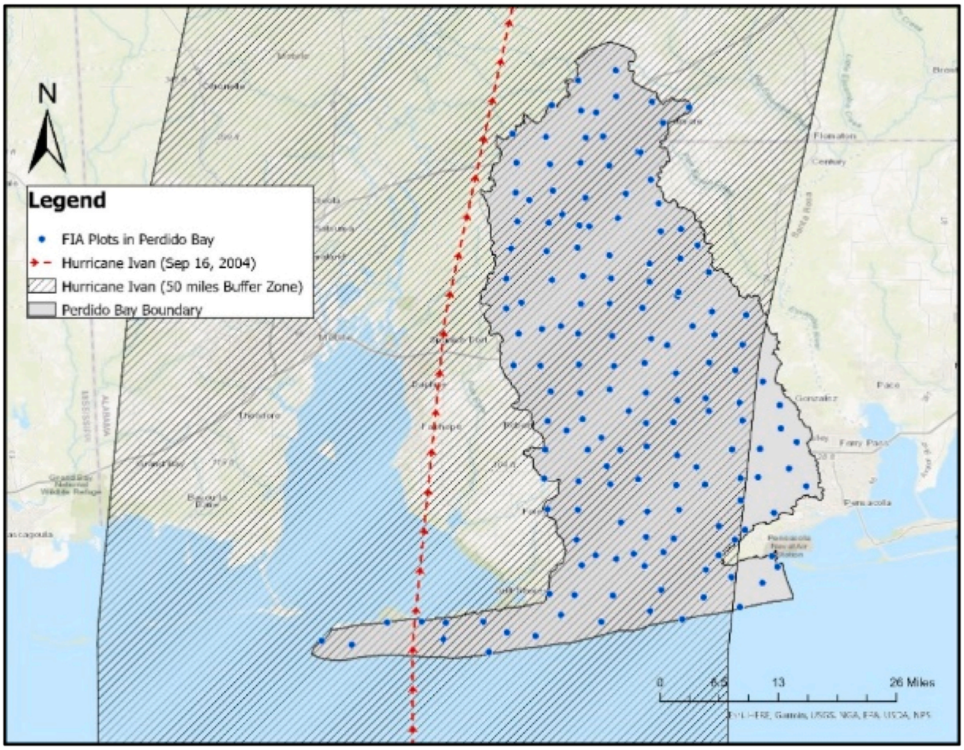

Fig. 1. Blue dots represent Forest Inventory and Analysis (FIA) plots in the Perdido Bay watershed. The survey cycle is 2001–2007.

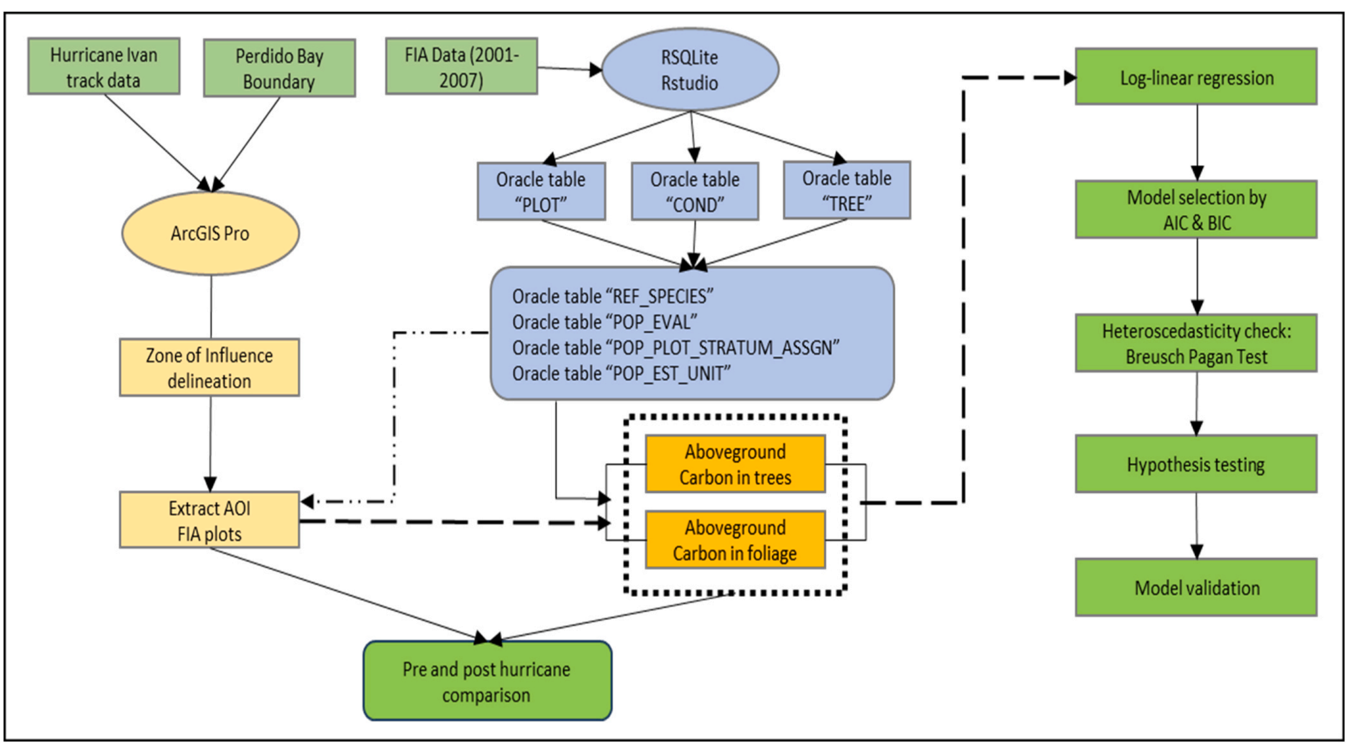

Fig. 2. Process flow diagram of processing FIA data from SQL database to regression-friendly data format.csv files. The dotted line with the arrow shows the intermediate process in the flow diagram.

obtaining comprehensive and comparable information on timber resources for all parts of the country (O'Connell and Conkling, 2016; Oswalt et al., 2018; Pugh et al., 2018). FIA inventories are commonly designed to meet the specified sampling errors at the State level at the 67 % confidence limit (one standard error) (O'Connell and Conkling, 2016). We followed the FIA sampling errors for the southern region to estimate aboveground carbon across the Perdido Bay watershed.

2.3. Aboveground carbon calculation for trees and foliage

The average diameter of each sampled plot was used to estimate the aboveground biomass in bole, stump, sampling, top, and foliage. In FIA data processing, the aboveground biomass amount of individual tree in the sampled plot was expanded to per hectare values using the TPA_UNADJ, a constant derived from the plot size (14.8 for trees sampled in subplots and 185.2 for trees sampled in microplots) (O'Connell and Conkling, 2016). Then, a population expansion factor was applied, which represents a stratum divided by the number of sampled plots in that stratum (Bechtold and Patterson, 2005; Bechtold and Scott, 2005). To calculate aboveground biomass in tree (bole, stump, sampling and top) and foliage, we used the component ratio method (CRM), which involves computing the dry weight of individual components before estimating the total aboveground or belowground biomass (Heath et al. 2009). This CRM method is based on calculating the biomass of the entire tree (total aboveground biomass), merchantable bole (including bark), and belowground biomass following Eq. (1) (Jenkins et al. 2003). We used the biomass conversion factor from Petersson et al. (2012) in our analysis to determine the dry-weight carbon values for aboveground carbon estimation.

$$\textit{Aboveground Carbon in Trees} = 0.5*(\exp(\textit{Jenkins\_Total\_B1} + \textit{Jenkins\_Total\_B2} * \ln(\textit{Dia}*2.54)) * 2.2046) \tag{1}$$

where *aboveground carbon in trees* = Total aboveground carbon (metric tons/ha) in bole, stump, top, sapling and foliage for trees 2.5 cm DBH or larger, *Jenkins_Total_B1* = Parameter estimate β_0 for hardwood, softwood and woodland species, *Jenkins_Total_B2* = Parameter estimate β_1 for hardwood, softwood and woodland species, *Dia* = Diameter-at-breast height (DBH) in cm.

In addition to PLOT, COND, and TREE table database, we extracted three more database tables; *Reference Species* ('REF_SPECIES'), *Population Evaluation* ('POP_EVAL'), and *Population Plot Stratum Assignment* ('POP_PLOT_STRATUM_ASSGN') to calculate aboveground carbon excluding foliage using (O'Connell and Conkling, 2016). This equation excludes foliage of live trees with a diameter at breast height (DBH) $\geq$ 2.5 cm, and dead trees with a DBH $\geq$ 12.7 cm. Finally, we calculated the aboveground carbon (metric tons/ha) by multiplying TPA_UNADJ and the population expansion factor following in O'Connell and Conkling, (2016).

$$\textit{Aboveground Carbon in Trees without Foliage} = 0.5*(\textit{Drybio\_Bole} + \textit{Drybio\_Stump} + \textit{Drybio\_Top} + \textit{Drybio\_Sapling} + \textit{Drybio\_Wdld\_Spp}) \tag{2}$$

where *aboveground carbon in trees without foliage* = Total aboveground carbon (metric tons) in bole, stump, top and sapling for trees 2.5 cm DBH or larger, *Drybio_Bole* = Oven dry biomass (metric tons) of sound wood in live and dead trees, including bark, from a 30 cm stump to a minimum 10 cm top diameter of the central stem, *Drybio_Stump* = Oven dry biomass (metric tons) of the trees from the ground to the bottom of the merchantable bole (i.e., below 30 cm), *Drybio_Top* = Oven dry biomass (metric tons) of the portion of the stem above the merchantable bole (i.e., above the 10 cm top diameter), and all branches; excludes foliage, *Drybio_Sapling* = Oven dry biomass (metric tons) of the aboveground portion, excluding foliage, of live trees (timber species only) with a diameter from 2.5 to 12.5 cm, *Drybio_Wdld_Spp* = Oven dry biomass (metric tons) of the aboveground portion of a live or dead tree, excluding foliage, the tree tip (top of the tree above 3.8 cm in diameter), and a portion of the stump from ground to diameter at root collar (DRC). We utilized Eqs. (1) and (2) to compare the impact of Hurricane Ivan on aboveground carbon in trees with foliage and without foliage.

2.4. Log-linear regression

Log-linear regression model transforms variables where a non-linear relationship exists between the independent and dependent variables, preserving the linear model characteristics (Miller, 1984; Benoit, 2011). This transformation helps to account for non-linear relationships in the data and results in a more accurate prediction of those relationships (Benedetti and Brown, 1978). In log-linear regression, the model is specified as:

$$Ln\ (Y) = \beta_0 + \beta_1 X_1 + \beta_2 X_2 + \ldots + \beta_p X_p + \varepsilon \tag{3}$$

where Y is the dependent variable, $X_1, X_2, \ldots, X_p$ are the independent variables, β_0 is the intercept, $\beta_1, \beta_2, \ldots, \beta_p$ are the coefficients or parameters that describe the relationship between the independent and dependent variables, and ε is the error term- indicate the uncertainty in the regression model. We decomposed Eq. (3) to derivate our log-linear equation for aboveground carbon in Eq. (4).

$$\textit{Log (Aboveground Carbon in trees/in trees without foliage)} = \beta_0 + \beta_1 * \textit{Inventory Year} + \beta_2 * \textit{Height} + \beta_3 * \textit{Diameter} + \beta_4 * \textit{Stand Age} + \beta_5 * \textit{Elevation} + \beta_6 * \textit{Plot Affected Status} + \beta_7 * \textit{Soil Physiographic Zone} + \beta_{10} * \textit{Stand Type} + \varepsilon \tag{4}$$

where Log (Aboveground Carbon in trees/in trees without foliage) = Total aboveground carbon (metric tons) in bole, stump, top and sapling for trees 2.5 cm DBH or larger, β_0 is the intercept, *Inventory Year* stands for the year that best represents when the inventory data were collected using code INVYR, *Height* is the total height (meter) of a sample tree from the ground to the tip of the apical meristem using code HT, *Diameter* is the current diameter (m) of the sample tree at the point of diameter measurement at either diameter-at-breast height (DBH) or at root collar (DRC) using code DIA, *Stand Age* is field recorded stand age (year) in annual inventory using stand age code STDAGE, *Elevation* is the distance (meter) the plot is located above sea level using code ELEV, *Plot Affected Status* is the condition of the plot whether it is affected by hurricane or other weather related damages in the field at the time of plot measurement using disturbance class code DSTRBCD1. A disturbance is recorded if the area affected by any natural or human-caused disturbance is at least 1.0 acre in size. Additionally, disturbance codes require "significant threshold" damage, which implies mortality and/or damage to 25 % of all trees in a stand or 50 % of an individual species' count. The year in which the disturbance occurred is also recorded., *Soil Physiographic Zone* is the general effect of land form, topographical position, and soil on moisture available to trees using physiographic class code PHYSCLCD, *Stand Type* is dominant tree species (softwood or hardwood) in a given plot using forest type code FORTYPCD and species group code SPGRPCD. β_1 , β_s……… β_{10} are coefficients of the mentioned variables for Eq. (4), and ε is the error term- indicate the uncertainty in the regression model.

Since the presence of heteroskedasticity makes the least-squares standard errors incorrect, we used “sandwich” package in R statistical software to adjust heteroskedasticity errors in our model (Zeileis, 2004; Zeileis et al. 2020). We used the most common robust type standard errors *vcovHC (type = "HC1")* in our analysis. HC1 applies a degree of freedom-based correction, (n−1)/(n− k) where n is the number of observations and k is the number of explanatory or predictor variables in the model (Achim et al. 2022). We used the *coeftest()* function to estimate heteroskedasticity-adjusted standard errors in our models.

2.5. Model selection through goodness of fit and heteroscedasticity test

For our model selection, we devised four different log-linear regression models (Table 1); consider '*inventory year*' as fixed effects across all models. For Model 1, we used all variables (*'height', 'diameter', 'plot affected status', 'stand age', 'elevation', 'soil physiographic zone', 'stand type'*) as variable effects except '*inventory year*'. In Model 2, we multiplied the average tree '*height*' and '*stand age*' to observe the joint effects of two variables in the model. We considered the '*basal area*' as a block variable in Model 3 to control for sources of variability across FIA data and oversee the character of multicollinearity with tree '*height*' and

Table 1
Models used to identify the "best" in model selection step fitting best regression model for aboveground carbon.

Log-linear regression for aboveground carbon in trees (bole, stump, top, sapling and foliage)	Model
log (aboveground carbon in trees) ~ $\beta_0 + \beta_1$ * Year + β_2 * Height + β_3 * Diameter + β_4 * Plot Affected Status + β_5 * Stand Age + β_6 * Elevation + β_7 * Soil Physiographic Zone + β_8 * Stand Type	1
log (aboveground carbon in trees) ~ $\beta_0 + \beta_1$ * Year + β_2 * Diameter + β_3 * Plot Affected Status + β_4 * Stand Age + β_5 * Elevation + β_6 * Soil Physiographic Zone + β_7 * Stand Type	2
log (aboveground carbon in trees) ~ $\beta_0 + \beta_1$ * Year + β_2 * Diameter + β_3 * Plot Affected Status + β_4 * Height * Stand Age + β_5 * Elevation + β_6 * Soil Physiographic Zone + β_7 * Stand Type	3
log (aboveground carbon in trees) ~ $\beta_0 + \beta_1$ * Year + β_2 * Diameter + β_3 * Plot Affected Status + β_4 * Height + β_5 * Stand Age + β_6 * Elevation + β_7 * Soil Physiographic Zone + β_8 * Stand Type + β_9 * Basal Area	4
Log-linear regression for aboveground carbon in trees without foliage	**Model**
log (aboveground carbon in trees without foliage) ~ $\beta_0 + \beta_1$ * Year + β_2 * Height + β_3 * Diameter + β_4 * Plot Affected Status + β_5 * Stand Age + β_6 * Elevation + β_7 * Soil Physiographic Zone + β_8 * Stand Type	1
log (aboveground carbon in trees without foliage) ~ $\beta_0 + \beta_1$ * Year + β_2 * Diameter + β_3 * Plot Affected Status + β_4 * Stand Age + β_5 * Elevation + β_6 * Soil Physiographic Zone + β_7 * Stand Type	2
log (aboveground carbon in trees without foliage) ~ $\beta_0 + \beta_1$ * Year + β_2 * Diameter + β_3 * Plot Affected Status + β_4 * Height * Stand Age + β_5 * Elevation + β_6 * Soil Physiographic Zone + β_7 * Stand Type	3
log (aboveground carbon in trees without foliage) ~ $\beta_0 + \beta_1$ * Year + β_2 * Diameter + β_3 * Plot Affected Status + β_4 * Height + β_5 * Stand Age + β_6 * Elevation + β_7 * Soil Physiographic Zone + β_8 * Stand Type + β_9 * Basal Area	4

'*diameter*'; since '*basal area*' is derived from DBH of the tree. For Model 4, we removed the variable '*height*' from the model to see the effect of tree '*height*' in our regression model comparison. We used four different goodness of fit tests to select the best model to determine whether a set of observed values match those expected under the best model; Residual Sum of Squares (RSS), Akaike Information Criterion (AIC), and Bayesian Information Criterion (BIC) (Steel RGD and Torrie, 1961; Burnham and Anderson, 2004; Chicco et al. 2021). We utilized these goodness-of-fit tests to select the best model for determining how well sample data fits a distribution from a population with a normal distribution. These tests also establish the discrepancy between the observed values and those expected of the model in a normal distribution case. After selecting the best model to describe aboveground carbon, we used the Breusch Pagan Test (BP Test) for the heteroscedasticity check in the selected model. Finally, we utilized Box-Cox transformation to address the heteroscedasticity in our model to stabilize the variance in residuals, lead to homoscedasticity, and make the FIA data to an approximate normal distribution (Gaudry and Dagenais, 1979; Nwakuya et al. 2018).

2.6. Model validation with performance metrics

After selecting our best model through goodness of fit, we determined the accuracy of the best model on predicting the outcome. We used k-fold cross-validation method using "caret" package in R to evaluate the model performance on different subsets of the training data and then calculate the average prediction error rate (Fushiki, 2011; Wong and Yang, 2017; Jung, 2018). We randomly split the data set into k-subsets (or k-fold), reserved one subset and trained the model on all other subsets. Then, we evaluated the model on the reserved subset and recorded the prediction error. This process is repeated until each of the k subsets has served as the test set. Finally, we computed the average of the k recorded errors; a cross-validation error serving as the performance metric for the model (Rodríguez et al. 2010). We utilized three statistical performance matrices for k-fold cross-validation for our selected model; R-squared (R^2), Root Mean Squared Error (RMSE), and Mean Absolute Error (MAE). R-squared measures the extent to which changes in the dependent variable (aboveground carbon in trees/in trees without foliage) can be predicted by changes in the independent variables (inventory year, height, diameter, plot affected status, stand age, elevation, soil physiographic zone, and stand type). Higher R-squared values indicate a better fit of the regression model to the data (Steel RGD and Torrie, 1961). RMSE measures the average prediction error made by the model in predicting the outcome for an observation. The lower the RMSE, the better the model. Lastly, MAE corresponds to the average absolute difference between observed and predicted outcomes. The lower the MAE, the better the model (Gunasegaran and Cheah, 2017; Pohjankukka et al. 2017).

3. Results

3.1. Aboveground carbon scenarios before and after Hurricane Ivan

We compared the average aboveground carbon in pre- and post-hurricane periods with different FIA data variables (stand type, stand size, physiographic class, height and stand age). Supplementary Table T1 shows the '*county*' and '*stand type*' wise plot affected status, where about 94 % of FIA plots were affected by Hurricane Ivan in 2004. FIA plots in Baldwin and Escambia County were affected most by Hurricane Ivan, with 70 % and 29 % plots, respectively. Escambia County in Alabama, located outside the hurricane influence zone (80 km), survived with most of the plots. Supplementary Figure F1 shows county-wise aboveground carbon distribution in trees (top, bole, stump, sapling) and in foliage before and after the hurricane. Our study found that the average aboveground carbon in trees in Baldwin County was about 87.94 metric tons/ha before the hurricane and decreased to 70.06 metric tons/ha after Hurricane Ivan. Aboveground carbon in foliage was observed with a decrease from 7.19 metric tons/ha to 5.65 metric tons/ha after the hurricane. Due to the unavailability of FIA data in Escambia (AL) County between 2004 and 2007, it was difficult to estimate aboveground carbon change immediately after the hurricane. We used the spatial interpolation technique to estimate the aboveground carbon between 2004 and 2007 for Escambia (AL) county. Our findings, however, indicated a significant decline that suggested the hurricane might have had an effect on aboveground carbon. After the hurricane, aboveground carbon in trees in Escambia County dropped from 130.78 metric tons/ha to 65.64 metric tons/ha. Correspondingly, aboveground carbon in foliage decreased from 4.75 metric tons/ha to 2.94 metric tons/ha in the post-hurricane period. Overall, aboveground carbon decreased from 101.51 metric tons/ha to 81.45 metric tons/ha (Fig. 3). The carbon in bole decreased markedly from 62.06 to 47.89 metric tons/ha in the post-hurricane period. Carbon decreased by about 1.16 metric tons/ha and 2.52 metric tons/ha, respectively, in stump and foliage in the post-hurricane period.

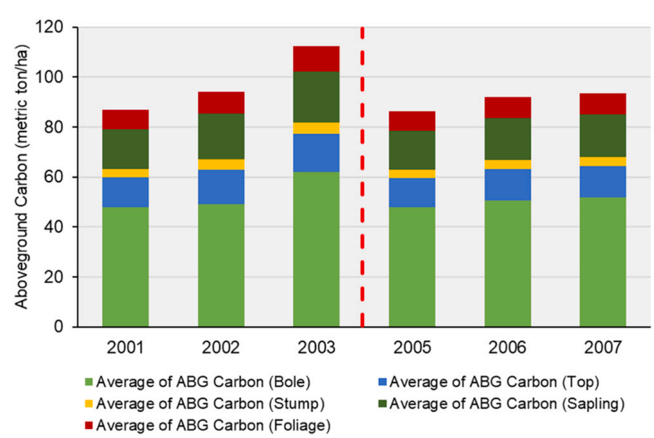

Fig. 3. Change of aboveground carbon in bole, stump, top, sapling, and foliage (metric tons/ha) before and after Hurricane Ivan. Red dotted line shows the intervention by Hurricane Ivan in 2004. ABG stands for aboveground carbon.

Fig. 4 shows the change of average aboveground carbon changes before and after Hurricane Ivan as per '*stand type*' (hardwood, mixed, and softwood) and '*stand size*' (large, medium, and small diameter). Since the plots numbers are different over the inventory years, our result revealed disproportionate changes in aboveground carbon over '*stand type*' and '*stand size*'. Plots with hardwoods were affected the most, as the average carbon decreased from 137.96 metric tons/ha to 40.51 metric tons/ha. Average carbon on mixed plots decreased from 101.41 metric tons/ha to 83.58 metric tons/ha. Plots with hardwood (*Liquidambar styraciflua* ~ Sweetgum, *Quercus texana* ~ Nuttall oak, *Quercus phellos* ~Willow oak) and mixed (hardwoods + softwoods) observed a carbon decrease (11.45 % and 3.66 %, respectively) at the end of post-hurricane period. However, more carbon (8.34 % increase) was observed in softwoods (*Pinus taeda (*loblolly pine), *Pinus elliottii* (slash pine), *Pinus clausa* (sand pine), and *Pinus palustris* (longleaf pine)) in post-hurricane inventory in 2005. The average carbon decrease rate in large and medium diameter trees was respectively 6.67 % and 5.43 % higher than small diameter trees due to the greater number of dead trees in the inventory year 2006. Foliage decreased in large- and medium-diameter stand size classes. However, stand class with small-diameter trees increased from 5.45 metric tons/ha to 12.42 metric tons/ha in the post-hurricane period.

Fig. 5 provides an illustration of how trees with different heights and stand ages were impacted by the hurricane. Plots containing relatively taller trees experienced significant ($p \leq 0.05$) carbon loss from the hurricane, primarily due to the higher carbon content in the 'bole', 'stump', 'top', and 'sapling', resulting in more carbon being stored in the 'foliage'. Among the relatively taller trees, those with heights ranging from 15 m to 20 m exhibited a sharp decrease in average aboveground carbon from 166.65 metric tons/ha before 2004–72.73 metric tons/ha after 2004. Specifically, average carbon in 'saplings' and 'bole' of taller and larger trees decreased by 73.34 % (from 34.16 metric tons/ha to 9.60 metric tons/ha) and 64.44 % (from 103.20 metric tons/ha to 38.07 metric tons/ha), respectively, compared to the pre-hurricane period. However, average carbon in 'foliage' increased from 12.69 metric tons/ha to 22.02 metric tons/ha, indicating the regeneration of tree leaves and branches. Regarding 'stand age', plots with a stand age of less than 25 years were the most affected, experiencing a decrease in average carbon from 126.91 metric tons/ha to 50.08 metric tons/ha after the hurricane. Similarly, plots with trees of middle age (26 years to 50 years) showed a similar trend, while relatively older trees (51 years to 75 years) gained more than 50 % carbon after the post-hurricane period. Our analysis found that carbon in the top of the trees increased from 25.18 metric tons/ha to 37.32 metric tons/ha, and foliage carbon increased from 12.69 metric tons/ha to 20.94 metric tons/ha after the hurricane.

Fig. 6 illustrates that average carbon decreased after the hurricane regardless of the physiographic zone. Plots located in bays and wet pocosins, which are low, wet, and boggy sites characterized by peaty or organic soils, were the most affected. The carbon in the tree 'bole' and 'sapling' decreased by 46.42 % and 46.17 %, respectively, compared to the pre-hurricane period. Additionally, plots in deep sands, flatwoods, and bottomlands also experienced decreases in average carbon, including carbon in 'foliage', which decreased from 82.10 metric tons/ha to 57.24 metric tons/ha, 64.62 metric tons/ha to 48.04 metric tons/ha, and 96.94 metric tons/ha to 84.20 metric tons/ha, respectively. On the other hand, plots in rolling uplands and small drains were less affected, as their carbon profiles remained relatively stable. However, there was a decrease of 29.65 metric tons/ha in 'sapling' carbon in small drains after the hurricane.

3.2. Regression diagnostics from model selection

Fig. 7 presents log-linear regression models for estimating aboveground carbon in trees (bole, stump, top, and sapling) and foliage. The results indicate that '*height*', '*physiographic class*', '*field age*' and '*stand type*' variables are statistically significant ($p \leq 0.05$) for estimating carbon in trees, while '*height*', '*field age*', '*stand size*', and '*stand type*' are statistically significant for estimating carbon in foliage. Table 2 shows our goodness-of-fit tests diagnostics; these tests selected Model 3 as the best for estimating aboveground carbon in trees with foliage and without foliage. The lower RSS of Model 3 indicates a better fit of the model to the observed data, as it represents smaller errors in prediction. Lower AIC and BIC values of Model 3 indicate a better-fitting model with appropriate complexity.

Table 3 shows the model validation results with three different performance metrices: R^2, RMSE and MAE. In Model 3 higher R^2 suggests that a larger proportion of the variability in the dependent variable ('*aboveground carbon*') has been accounted for by the independent variables (*'height', 'physiographic class', 'field age', 'stand size' and 'stand type'*). This compliments Model 3 with more accurate predictions than other models. Correspondingly, lower RMSE and MAE values in Model 3 indicate that the predictions are closer to the actual observed values than other models.

Table 4 shows the Breusch-Pagan (BP) heteroscedasticity test for Model 3. Since both the p-values in the models are not less than $\alpha = .05$, hence we assume that homoscedasticity is present in our selected model. Regression diagnostics show no pattern in the residual plot of the model (Supplementary Figures F2 & F3). This suggests we can assume a linear relationship between the predictors ('aboveground carbon in trees' and 'aboveground carbon in trees without foliage') and the response variables (*'year', 'diameter', 'plot affected status', 'height', 'stand age', 'elevation', 'soil physiographic zone', 'stand type'*).

Fig. 8 displays parameter estimates ($p \leq 0.05$) from the best model for quantifying aboveground carbon in trees and foliage. Our findings reveal a negative trend in aboveground carbon productivity following the hurricane. Aboveground carbon in trees and foliage started decreasing after Hurricane Ivan, with a higher rate of decrease observed in 'foliage' compared to trees. More dead trees were reported in the 2005

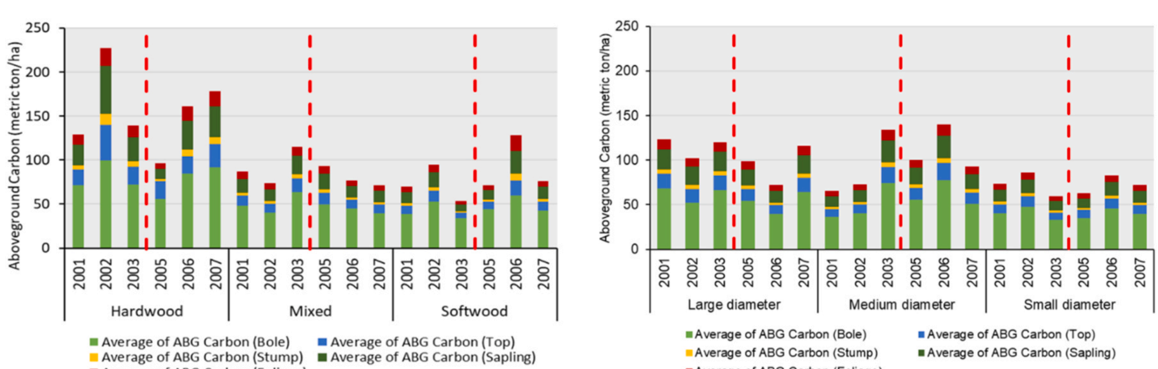

Fig. 4. Change of aboveground carbon in bole, stump, top, sapling and foliage (metric tons/ha) before and after Hurricane Ivan as per stand type and stand size. Red dotted line shows the intervention by Hurricane Ivan in 2004. ABG stands for aboveground carbon.

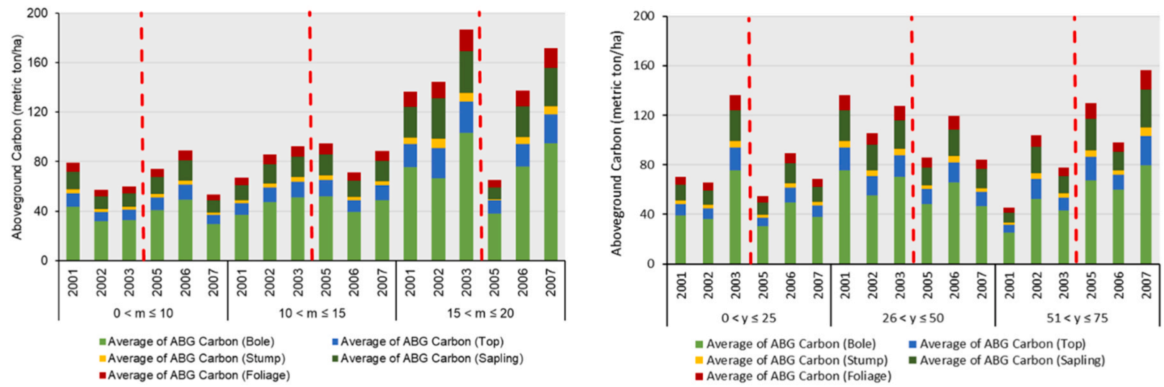

Fig. 5. Change of aboveground carbon (metric tons/ha/year) in trees in trees and foliage related to height (in meters) and stand age (in years) of the sampled plots before and after Hurricane Ivan. Red dotted line shows the intervention by Hurricane Ivan in 2004.

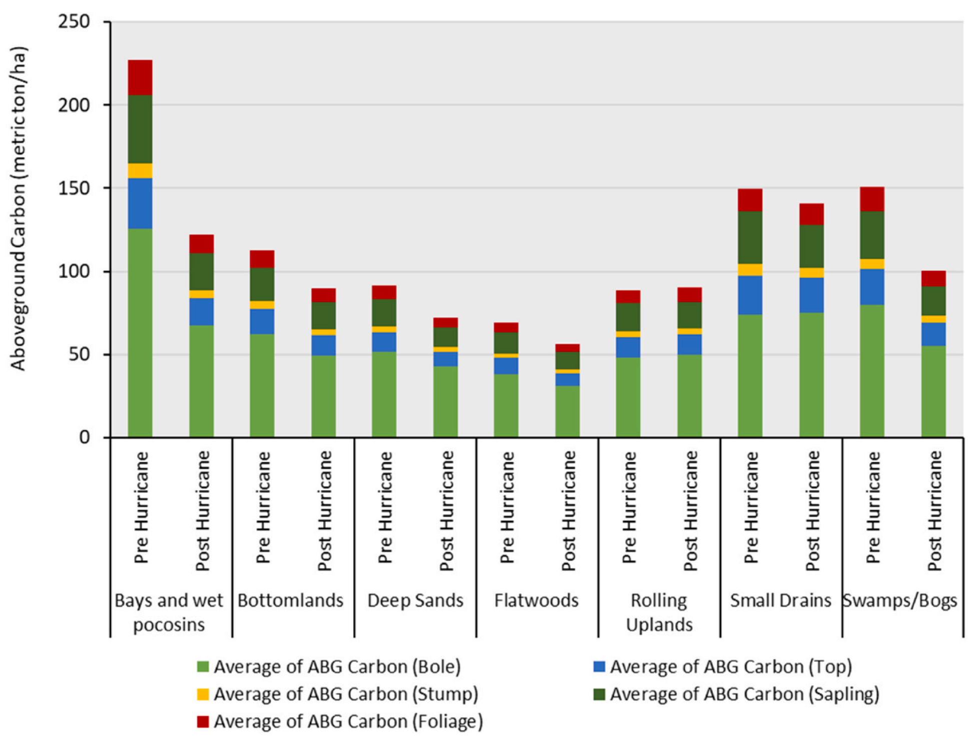

Fig. 6. Distribution of average aboveground carbon changes before (2001–2003) and after (2005–2007) Hurricane Ivan period considering physiographic classes available in the Gulf Coast.

annualized data, resulting in a 19 % carbon decrease compared to 2001. Plots dominated with softwood '*stand type*' exhibited 48.30 % higher aboveground carbon compared to hardwood '*stand type*' and 24.25 % higher than '*mixed*' stand type. Carbon in medium-diameter stands (28 ≥ DBH ≥ 12.5 cm) and small-diameter stands (< 12.5 cm DBH) changed by 15.40 % and 9.25 %, respectively, compared to trees with large diameter (≥ 28 cm DBH for 'hardwoods' and ≥ 22 cm DBH for 'softwoods' as per FIA). Aboveground carbon in the foliage was higher in plots with medium-diameter stands compared to large-diameter stands (Fig. 9). Aboveground carbon was higher in rolling uplands (58.78 %) and flatwoods (63.25 %) compared to bays and wet pocosins. The interaction variable '*height * field age*' shows a significant change in the foliage loss; about 65.06 % increase in foliage loss was reported in the study period. The '*elevation*' of plots, '*field age*', and '*height*' of trees in the affected plots showed minor impacts (~0.01 % - 2.20 %) on the overall carbon profile in the model during the study period.

4. Discussion

4.1. Forest structure and hurricane effects on aboveground carbon

Pre-hurricane stand characteristics were important factors that determined the vulnerability of the trees to hurricane damage. Hurricane Ivan showed a disproportionate impact on plots with large and small-diameter trees, as well as softwood-dominated stands. In the affected plots, the average aboveground carbon loss was estimated to be about 26 metric tons/ha. Our results were consistent with previous research that found hurricanes caused the most damage to large-diameter stands in major forest types in the southeastern United States (Platt et al. 2000; Ojha et al. 2020; Zampieri et al. 2020; Id et al. 2021). Forest management practices were introduced to help mitigate aboveground carbon loss, yet subsequent effects of hurricanes triggered long-term challenges for the landowners (Ameray et al. 2021). For example, Chevalier et al. (2022) applied experimental forest

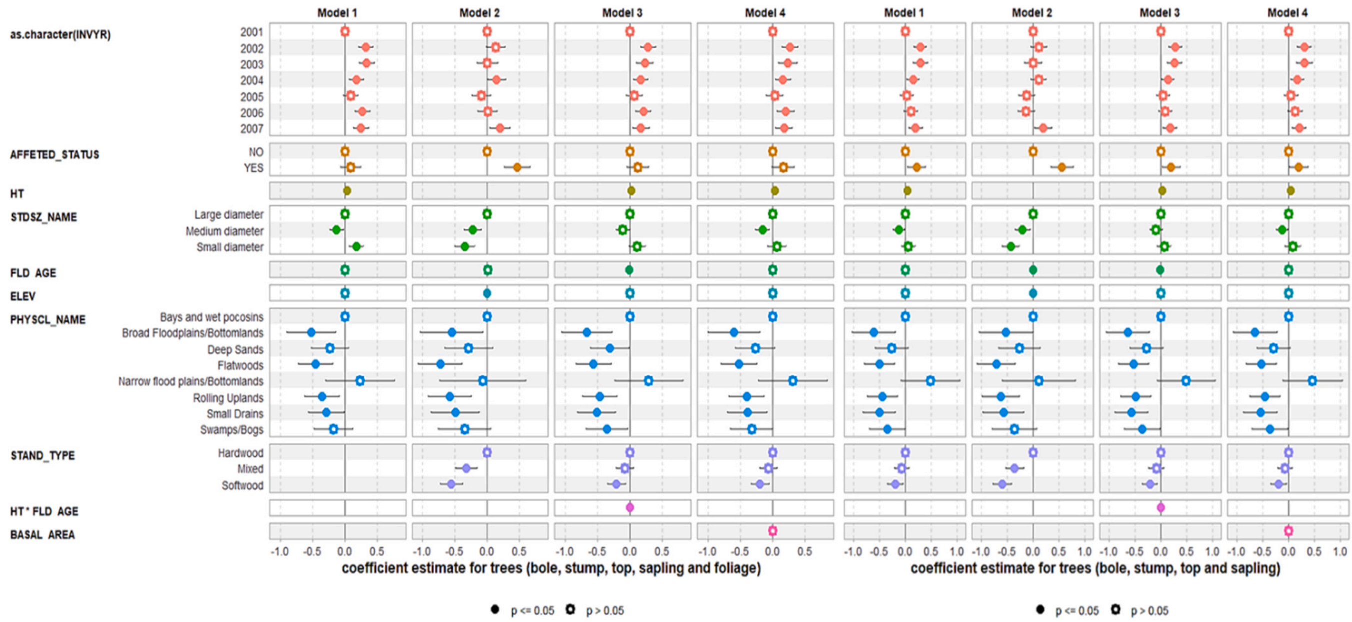

Fig. 7. Log-linear model using different biophysical parameters and a fixed effect (inventory year "INVYR"); *AFFETED_STATUS* is the condition of the plot whether is it affected by hurricane or other weather damages using DISTRBNCD variable in FIA database, *HT* is the total height (meter) of a sample tree from the ground to the tip of the apical meristem, *ELEV* is the distance (meter) the plot is located above sea level, *PHYSCL_NAME* is the general effect of land form, topographical position, and soil on moisture available to trees, *STAND_TYPE* is dominant tree species (softwood or hardwood) in a given plot and *BASAL AREA* is the square meter per hectare of all live trees in a given plot. All models were performed with 95 % CIs. The coefficient estimates on the left of "0" shows the negative change of the variables in the model.

Table 2
Diagnostics of goodness of fit tests of four log-linear regression models to estimate aboveground carbon.

	Aboveground carbon in trees (bole, top, stump, sapling, and foliage)			Aboveground carbon in trees (bole, top, stump and sapling)		
Model	RSS	AIC	BIC	RSS	AIC	BIC
1	0.662	3937.200	4064.810	0.704	4178.830	4306.430
2	0.825	4793.410	4915.490	0.879	5042.510	5164.590
3	***0.657***	***3909.340***	***4042.460***	***0.701***	***4165.500***	***4298.630***
4	0.662	3938.270	4071.390	0.704	4180.230	4313.360

Table 3
Model performance matrices of K-fold cross-validation.

	Aboveground carbon in trees (bole, top, stump, sapling, and foliage)			Aboveground carbon in trees (bole, top, stump, and sapling)		
Model	R^2	RMSE	MAE	R^2	RMSE	MAE
1	0.43329	0.66401	0.51238	0.43328	0.70630	0.53932
2	0.11736	0.82923	0.62721	0.11756	0.88233	0.68788
3	0.44168	0.65928	0.50811	0.43756	0.70365	0.53790
4	0.43263	0.66435	0.51249	0.43294	0.70652	0.53943

Table 4
Breusch-Pagan (BP) heteroscedasticity test for the selected model.

Selected Model	BP test statistic	df	p-value	Status
Model 3 – log (aboveground carbon in trees) ~ $\beta_0 + \beta_1$ * Year + β_2 * Diameter + β_3 * Plot Affected Status + β_4 * Height * Stand Age + β_5 * Elevation + β_6 * Soil Physiographic Zone + β_7 * Stand Type	324.2	22	0.05 < 0.89	Homoscedastic
Model 3 – log (aboveground carbon in trees without foliage) ~ $\beta_0 + \beta_1$ * Year + β_2 * Diameter + β_3 * Plot Affected Status + β_4 * Height * Stand Age + β_5 * Elevation + β_6 * Soil Physiographic Zone + β_7 * Stand Type	323.1	22	0.05 < 0.88	Homoscedastic

management techniques in a tropical forest in Puerto Rico by trimming the canopy to regenerate aboveground carbon but reported continued carbon loss in larger trees after Hurricane Maria. This suggests that even though management practices may aid in recovery, large trees still face challenges in retaining aboveground carbon after severe hurricane events. Correspondingly, younger and smaller trees have a higher ratio of living sapwood to heartwood than older trees, which makes them elastic and flexible (Paul McLean et al. 2011; Sharma et al. 2018; USDA, 2021). The elasticity of the smaller softwoods stands out as potentially resistant to aboveground carbon loss in small-diameter trees. In our case, this resulted in about 1.24 % more aboveground carbon decrease in plots with large-diameter trees than in plots with small-diameter trees.

Stand age is an important factor that influences the amount of aboveground carbon in trees and foliage. As stands age, trees tend to grow taller and increase in diameter, leading to greater overall biomass and carbon storage. This results in a greater height-to-diameter (h:d) ratio, which lowers their stability and increases vulnerability to wind-throw overturning (Xi et al. 2008b). Our findings aligned with the results from Valinger and Fridman (2011) and Xi et al. (2008a), which

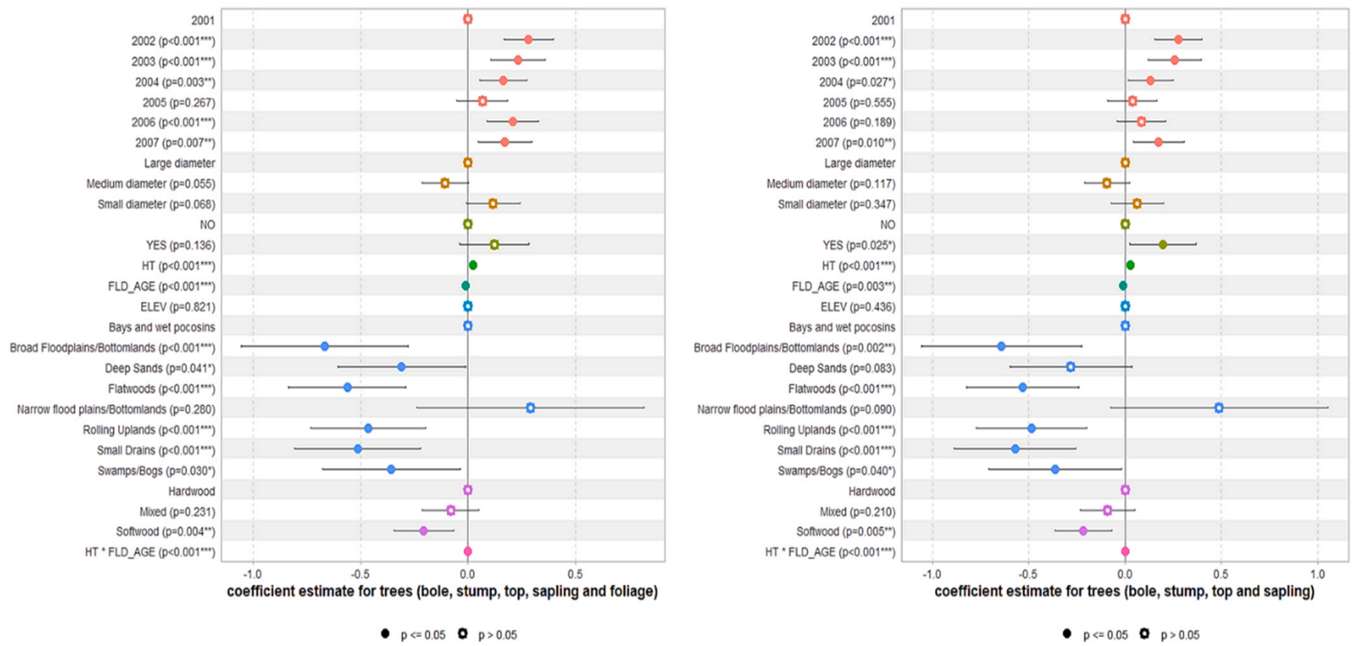

Fig. 8. Coefficients of the best log-linear regression model (Model 3) for aboveground carbon (metric tons/ha) with and foliage. Error bars show the significant difference between plot samples and the variability of standard deviation around the mean value. Models were performed with 95 % CIs. The coefficient estimates on the left of "0" shows the negative change of the variables in the model.

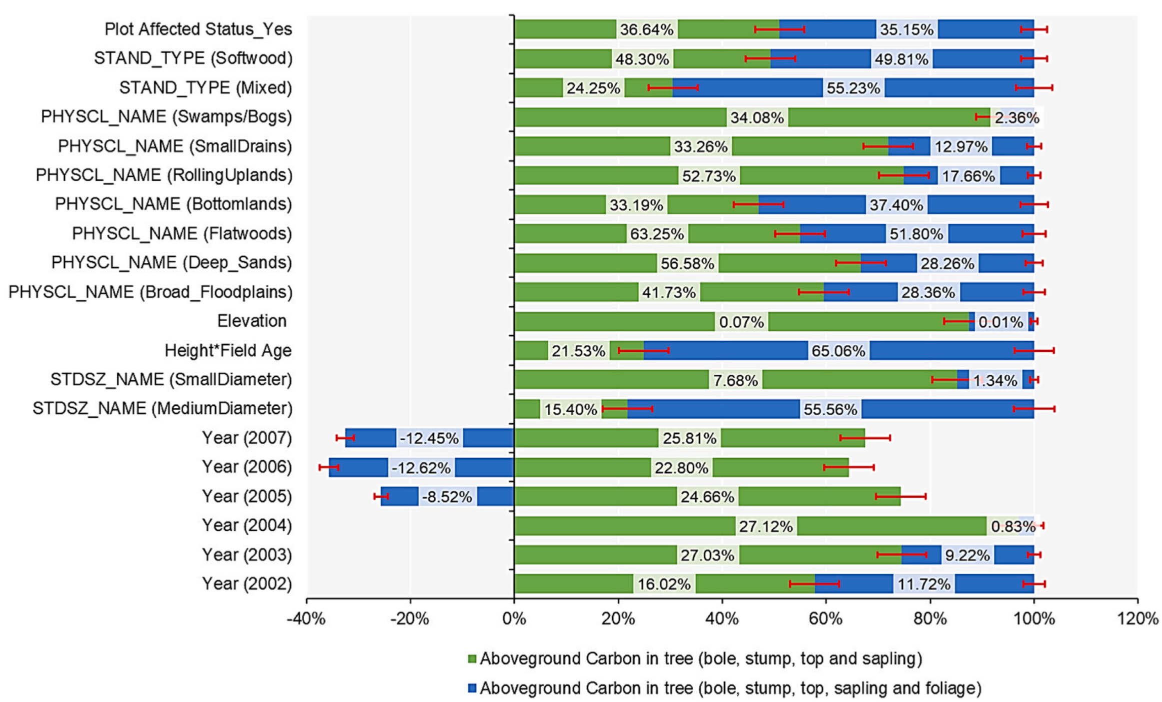

Fig. 9. Estimates of relative changes in aboveground carbon (metric tons/ha) in trees and foliage (metric tons/ha) only compared to the year 2001. Error bars show the significant difference between plot samples and the variability of standard deviation around the mean value.

show that taller, older trees lower the stability of stands due to a lower ratio of living sapwood and their increased vulnerability to windthrow. Studies estimating aboveground carbon by physical characteristics of stands and a physiographic class of landform are very limited. Our study quantified the aboveground carbon in all physiographic classes available in Perdido Bay. Melson et al. (2011) estimated live tree carbon stored in the Pacific Northwest region using the height and DBH of the trees, but they did not report the tree carbon distribution across different physiographic soil types. Rivera-Monroy et al. (2019) and Castañeda-Moya et al. (2020) quantified how Hurricane Irma influenced soil nutrient pools, vertical accretion, and plant phosphorus uptake after its passage across the Florida Coastal Everglades in September 2017. However, they focused more on soil nutrients than aboveground carbon in trees and foliage.

Our study attempted to describe the distribution of aboveground carbon in rolling uplands, deep sands, swamps, bay and wet pocosins. Kuhn et al. (2021) estimated the volumetric change of biochemical properties (carbon, nitrogen, phosphorus, and sulfur) of soil in coastal wetlands after Hurricane Harvey in August 2017. They also reported the root biomass change both in marsh and mangrove stands, but their experimental plot was smaller compared to our study area. Their study did not quantify the aboveground carbon in marshlands. Our study created a scope of using physiographic classes to estimate aboveground carbon not only for overseeing a regional variance of carbon distribution across the stands but also for maintaining healthy vegetation after a major hurricane. The carbon stored in the plant foliage is a crucial component of the carbon cycle and essential to ecosystem functioning. Foliage carbon is instrumental in photosynthesis, in which plants use sunlight and carbon dioxide from the atmosphere to produce sugars, cellulose, and other organic compounds. However, while several studies (Ryan et al. 1997; Coulston et al. 2015; Lu et al. 2015; Hoover and Smith, 2021, 2023) focus on changes in aboveground carbon in trees, including the bole, top, stump, and sapling, the carbon stored in foliage is often overlooked.

4.2. Log-linear regression on estimating aboveground carbon

The general approach for modeling hurricane effects on aboveground carbon using log-linear regression is similar to that for estimating aboveground carbon but with the addition of hurricane-related predictor variables. In our case, the categorical predictor variables represented forest types, physiographic classes, stand size, or other qualitative factors that affect aboveground carbon stocks. Our study revealed a non-linear pattern in the association between the response variables (aboveground carbon with or without foliage) and the predictor variables. Hence, log-linear regression model offered a logarithmic transformation between the variables, which expected to be proportional or multiplicative. For example, one unit change in stand size with small diameter plots produced 7.6 % change in aboveground carbon in bole, stump, top, and sapling and a 1.3 % change in aboveground carbon in bole, stump, top, sapling, and foliage regardless of hurricane timeframe – assuming other variables are constant. Similarly, for medium-diameter plots, one unit change produced 15.4 % and 55.6 % change in aboveground carbon in trees and aboveground carbon in trees and foliage, respectively. This suggests that plots with medium-diameter stands have a greater possibility of losing aboveground carbon than that of small-diameter stands. Peneva-Reed et al. (2021) found that the initial reduction of carbon loss in the Ding Darling mangrove area caused by Hurricane Charley (2004) was between 0.5 % and 5.3 % under three different carbon loss scenarios; subtracted leaf biomass from the whole tree biomass, 15 % of total tree biomass lost and having only the biomass of the stem remaining. The approach they used in their study was similar to ours regarding the inclusion of foliage in carbon calculation before and after the hurricane event.

When we consider the '*inventory year*' as a predictor variable, the change of one unit of inventory year after Hurricane Ivan (2004) decreased 8.5 % in aboveground carbon in bole, stump, top, sapling, and foliage and 24.6 % increase in aboveground carbon in bole, stump, top, and sapling. Our findings from the yearly rate of changes in aboveground carbon are close to the findings from Griffiths and Mitsch (2021) – 7.2 % changes yearly after Hurricane Irma (2017). Their estimated aboveground carbon before (2013–2014) Hurricane Irma was about 97.8 metric tons/ha- similar findings (101.5 metric tons/ha) estimated in our analysis before Hurricane Ivan. Our log-linear regression model evaluated the significance level ($p < 0.05$) of the yearly FIA data which established the strong relationship between inventory year and aboveground carbon change. Delphin et al. (2013) added '*tree type*', '*height*', '*diameter*' and '*basal area*' in their analysis to estimate the forest damage from hurricanes in southwestern Florida. They considered these variables as direct drivers on aboveground carbon storage in their InVEST (Integrated Valuation of Ecosystem Services and Tradeoffs) model and decision tree analysis, however, they did not offer any statistical test for the variables. We included not only the heteroscedasticity test and model validation in our analysis but also frequently used statistical parameters – R^2, RMSE, RSS, etc. which gives us variables that are significantly important for our aboveground carbon estimation. For instance, in our case, '*stand type*' ($p < 0.05$) which referred to '*tree type*' in Delphin et al. (2013) played a pivotal role in our analysis. Plots with the softwood and mixed stands comparatively lost more carbon than hardwoods – 23.5 % more carbon lost in trees and 28.8 % more carbon lost in trees with foliage. The combined effect of '*height*' and '*field age*' variables showed a significant impact on changing aboveground carbon rather than considering them individually; more than 65 % of carbon increased in trees with foliage at the end of the study period.

Two main advantages of using log-linear regression are flexibility and interpretability (Haber, 1985; Smunt, 1999). Our regression model did not consider any local or regional scale variable, which restricted our aboveground carbon estimates to a certain geographic location. Peneva-Reed et al. (2021), Abdul-Hamid et al. (2022) and Pati et al. (2022) used allometric equations to estimate aboveground carbon for different tree species after natural intervention. However, allometric equations have some limitations, with limited geographic and size applicability, limited accuracy, and limited consideration of site-specific factors (Vorster et al. 2020). Log-linear regression has greater flexibility compared to locally developed allometric equations (Ma et al. 2021). Allometric equations assume a linear relationship between tree size and carbon stocks, which may not hold true for all tree species or all stages of tree growth. This can result in underestimation or overestimation of biomass or carbon stocks (Köhl et al. 2017). Since log-linear regression models can include more than one predictor variable, they may offer greater interpretability than allometric equations. This can help to account for the effects of these variables on aboveground carbon stocks, which may not be well represented by straightforward allometric equations.

5. Conclusion

Forests are crucial for mitigating climate change by absorbing carbon from the atmosphere and storing it in biomass and soils. However, climate change can increase the frequency and intensity of extreme weather events such as hurricanes, which can have significant impacts on forest structure and aboveground carbon stocks. Hurricanes can cause defoliation, damage or loss of trees, and soil erosion, which can alter ecosystem structure and function, reduce carbon sequestration, and contribute to climate change. Moreover, changes in forest structure and function due to hurricanes can affect the water balance of forests, affecting the evapotranspiration rates and leading to changes in regional climate patterns. It is therefore important to understand the interaction between forest structure, hurricanes, and climate change to predict the impacts of these disturbances on carbon stocks and climate and to develop effective management strategies to reduce the vulnerability of forests to hurricanes and maximize their capacity to sequester carbon and mitigate climate change.

To assess the impact of natural disasters such as Hurricane Ivan on aboveground carbon in coastal forests, log-linear regression modeling approach was adopted with categorical variables. This approach can estimate aboveground carbon in forests and identify the factors that influence carbon sequestration. Our study found that '*stand type*', '*height*', '*physiographic class*', and hurricane '*plot affected status*' of the FIA plots are statistically significant factors. The rate of aboveground carbon change in foliage is observed to be higher than that of trees, and foliage carbon is a major source of energy and nutrients for many organisms in ecosystems. Therefore, adding foliage carbon in the log-linear regression model provides another dimension to see the carbon dynamics after a major hurricane. We also found that the aboveground carbon decrease in '*hardwood*' stand type is more significant than in '*softwood*' stand type, varying by the predominant tree diameter of the stands.

Our study provides several conclusions that can be used as a basis for resistance, resilience, and adaptation of southern US coastal forests and of forests in other locations to the increased incidents of hurricanes and climate change. Forest management will benefit from an improved understanding of the mechanisms behind the resistance and resilience of forest stands and species to catastrophic wind. Our study also provides a framework for researchers and policymakers to assess the vulnerability of coastal forests and facilitate strategic planning to protect forests as carbon sinks. Future studies should include water level and storm surge information in the affected areas to examine how flooding and salinity affect coastal forests and marsh migration into inland areas. Modeling studies should evaluate the impacts of future storm surges, salinity, and land use changes on coastal forests to inform forest management. Since our current study did not explore the accounting of carbon growth due to replantation of softwood species, this could bring new avenues in sustainable forest management practices.

Funding source

Research reported in this publication was supported by the Gulf Research Program of the National Academies of Sciences, Engineering, and Medicine under award number 200011513. The content is solely the responsibility of the authors and does not necessarily represent the official views of the Gulf Research Program or the National Academies of Sciences, Engineering, and Medicine.

CRediT authorship contribution statement

Asiful Alam: Writing – review & editing, Writing – original draft, Validation, Software, Methodology, Formal analysis, Data curation. **Parag Kadam:** Methodology. **Puneet Dwivedi:** Writing – review & editing, Methodology, Conceptualization. **Andres Baeza-Castro:** Data curation. **Thomas Brandeis:** Methodology, Data curation.

Declaration of Competing Interest

The authors declare that they have no known competing financial interests or personal relationships that could have appeared to influence the work reported in this paper.

Data Availability

Data will be made available on request.

Acknowledgements

The authors are thankful to the scientists who provided their critical inputs to develop the research and participated in the research discussion for the successful completion of this research.

Appendix A. Supporting information

Supplementary data associated with this article can be found in the online version at doi:10.1016/j.foreco.2024.122067.

References

Abdul-Hamid, H., Mohamad-Ismail, F.N., Mohamed, J., et al., 2022. Allometric equation for aboveground biomass estimation of mixed mature mangrove forest. Forests 13, 1–18. https://doi.org/10.3390/f13020325.

Achim Z., Thomas L., Nathaniel G., Susanne K. (2022) Package "sandwich" Title Robust Covariance Matrix Estimators.

Ameray, A., Bergeron, Y., Valeria, O., et al., 2021. Forest carbon management: a review of silvicultural practices and management strategies across boreal, temperate and tropical forests. Curr. Rep. 7, 245–266. https://doi.org/10.1007/s40725-021-00151-w.

Bechtold W.A., Patterson P.L. (2005) The Enhanced Forest Inventory and Analysis Program-National Sampling Design and Estimation Procedures. Asheville, NC.

Bechtold W.A., Scott C.T. (2005) The Forest Inventory and Analysis Database Phase 2 (V 9). Washington DC.

Benedetti, J.K., Brown, M.B., 1978. Strategies for the selection of log-linear models. Int Biom. Soc. 34, 680–686.

Benoit K. (2011) Linear Regression Models with Logarithmic Transformations. London.

Blennow, K., Sallnäs, O., 2004. WINDA - A system of models for assessing the probability of wind damage to forest stands within a landscape. Ecol. Model. 175, 87–99. https://doi.org/10.1016/j.ecolmodel.2003.10.009.

Burnham, K.P., Anderson, D.R., 2004. Multimodel inference: understanding AIC and BIC in model selection. Socio Methods Res 33, 261–304. https://doi.org/10.1177/0049124104268644.

Castañeda-Moya, E., Rivera-Monroy, V.H., Chambers, R.M., et al., 2020. Hurricanes fertilize mangrove forests in the Gulf of Mexico (Florida Everglades, USA). Proc. Natl. Acad. Sci. USA 117, 4831–4841. https://doi.org/10.1073/pnas.1908597117.

Chambers, J.Q., Fisher, J.I., Zeng, H., et al., 2007. Hurricane Katrina's carbon footprint on U.S. Gulf Coast forests. Science 80 (318), 1107. https://doi.org/10.1126/science.1148913.

Chevalier, H., Brokaw, N.V.L., Ward, S.E., et al., 2022. Aboveground carbon responses to experimental and natural hurricane impacts in a subtropical wet forest in Puerto Rico. Ecosphere 13, e4041. https://doi.org/10.1002/ECS2.4041.

Chicco, D., Warrens, M.J., Jurman, G., 2021. The coefficient of determination R-squared is more informative than SMAPE, MAE, MAPE, MSE and RMSE in regression analysis evaluation. PeerJ Comput. Sci. 7, 1–24. https://doi.org/10.7717/PEERJ-CS.623.

Coulston J.W., Reams G.A. (2005) The effect of blurred plot coordinates on interpolating forest biomass: a case study.

Coulston, J.W., Wear, D.N., Vose, J.M., 2015. Complex forest dynamics indicate potential for slowing carbon accumulation in the southeastern United States. Sci. Rep. 5, 8002. https://doi.org/10.1038/srep08002.

Delphin, S., Escobedo, F.J., Abd-Elrahman, A., Cropper, W., 2013. Mapping potential carbon and timber losses from hurricanes using a decision tree and ecosystem services driver model. J. Environ. Manag. 129, 599–607. https://doi.org/10.1016/j.jenvman.2013.08.029.

Fushiki, T., 2011. Estimation of prediction error by using K-fold cross-validation. Stat. Comput. 21, 137–146. https://doi.org/10.1007/s11222-009-9153-8.

Gaudry, M.J.I., Dagenais, M.G., 1979. Heteroscedasticity and the use of Box-Cox transformations. Econ. Lett. 2, 225–229. https://doi.org/10.1016/0165-1765(79)90026-0.

GFDL (2023) Global Warming and Hurricanes – Geophysical Fluid Dynamics Laboratory. ⟨https://www.gfdl.noaa.gov/global-warming-and-hurricanes/⟩. Accessed 17 Nov 2023.

Griffiths, L.N., Mitsch, W.J., 2021. Estimating the effects of a hurricane on carbon storage in mangrove wetlands in southwest Florida. Plants 10. https://doi.org/10.3390/plants10081749.

Gunasegaran, T., Cheah, Y.N., 2017. Evolutionary cross validation. ICIT 2017 - 8th. Int Conf. Inf. Technol. Proc. 89–95. https://doi.org/10.1109/ICITECH.2017.8079960.

Haber, M., 1985. Maximum likelihood methods for linear and log-linear models in categorical data. Comput. Stat. Data Anal. 3, 1–10. https://doi.org/10.1016/0167-9473(85)90053-2.

Hanewinkel, M., Kuhn, T., Bugmann, H., et al., 2014. Vulnerability of uneven-aged forests to storm damage. Forestry 87, 525–534. https://doi.org/10.1093/forestry/cpu008.

Heath L.S., Hansen M.H., Smith J.E., et al (2009) Investigation into Calculating Tree Biomass and Carbon in the FIADB Using a Biomass Expansion Factor Approach.

Hoover, C.M., Smith, J.E., 2021. Current aboveground live tree carbon stocks and annual net change in forests of conterminous United States. Carbon Balance Manag 16 (1), 12. https://doi.org/10.1186/s13021-021-00179-2.

Hoover, C.M., Smith, J.E., 2023. Aboveground live tree carbon stock and change in forests of conterminous United States: influence of stand age. Carbon Balanc Manag 2023 181 18 (1), 11. https://doi.org/10.1186/S13021-023-00227-Z.

Houghton, R.A., House, J.I., Pongratz, J., et al., 2012. Carbon emissions from land use and land-cover change. Biogeosciences 9, 5125–5142. https://doi.org/10.5194/bg-9-5125-2012.

Id, A.S., Id, S.K.O., Dimov, L.D., Vogel, J.G., 2021. Long-term effects of catastrophic wind on southern US coastal forests. Lessons a Major Hurric. 27 (1) https://doi.org/10.1371/journal.pone.0243362.

IPCC (2014) Climate Change 2014: Synthesis Report.

IPCC (2015) Climate Change 2014 Synthesis Report. Geneva.

IPCC (2023) Summary for Policymakers: Synthesis Report.

Jehn, F.U., Kemp, L., Ilin, E., et al., 2022. Focus of the IPCC assessment reports has shifted to lower temperatures. Earth'S. Futur 10. https://doi.org/10.1029/2022EF002876.

Jenkins, J.C., Chojnacky, D.C., Heath, L.S., Birdsey, R.A., 2003. National-scale biomass estimators for United States Tree Species. Sci 49, 12–35.

Jung, Y., 2018. Multiple predicting K-fold cross-validation for model selection. J. Nonparametr. Stat. 30, 197–215. https://doi.org/10.1080/10485252.2017.1404598.

Kemp, L., Xu, C., Depledge, J., et al., 2022. Climate endgame: exploring catastrophic climate change scenarios. Proc. Natl. Acad. Sci. USA 119, 1–9. https://doi.org/10.1073/pnas.2108146119.

Köhl, M., Neupane, P.R., Lotfiomran, N., 2017. The impact of tree age on biomass growth and carbon accumulation capacity: a retrospective analysis using tree ring data of three tropical tree species grown in natural forests of Suriname. PLoS One 12, 1–17. https://doi.org/10.1371/journal.pone.0181187.

Kuhn, A.L., Kominoski, J.S., Armitage, A.R., et al., 2021. Buried hurricane legacies: increased nutrient limitation and decreased root biomass in coastal wetlands. Ecosphere 12. https://doi.org/10.1002/ecs2.3674.

LaPoint, E., 2005. Access and use of FIA data through FIA spatial data services. Proc. Fifth Annu. For. Inventory Anal. Symp. 199–202.

Lu, X., Kicklighter, D.W., Melillo, J.M., et al., 2015. Land carbon sequestration within the conterminous United States: regional- and state-level analyses. J. Geophys Res. Biogeosci 120, 379–398. https://doi.org/10.1002/2014jg002818.

Ma, J., Yuan, C., Zhou, J., et al., 2021. Logistic model outperforms allometric regression to estimate biomass of xerophytic shrubs. Ecol. Indic. 132, 108278 https://doi.org/10.1016/j.ecolind.2021.108278.

Melson, S.L., Harmon, M.E., Fried, J.S., Domingo, J.B., 2011. Estimates of live-tree carbon stores in the Pacific Northwest are sensitive to model selection. Carbon Balance Manag 6 (1), 16. https://doi.org/10.1186/1750-0680-6-2.

Miller, A.J., 1984. Selection of subsets of regression variables. J. R. Stat. Soc. 147, 389–425.

Murdiyarso, D., Purbopuspito, J., Kauffman, J.B., et al., 2015. The potential of Indonesian mangrove forests for global climate change mitigation. Nat. Clim. Chang 5, 1089–1092. https://doi.org/10.1038/nclimate2734.

National Weather Service (2005) Hurricane Ivan - September 16, 2004. ⟨https://www.weather.gov/mob/ivan⟩. Accessed 4 Apr 2023.

NCEI (2022) Billion-Dollar Weather and Climate Disasters | National Centers for Environmental Information (NCEI). ⟨https://www.ncei.noaa.gov/access/billions/⟩. Accessed 13 Jul 2022.

Negrón-Juárez, R., Baker, D.B., Zeng, H., et al., 2010. Assessing hurricane-induced tree mortality in U.S. Gulf Coast forest ecosystems. J. Geophys Res. Biogeosciences 115. https://doi.org/10.1029/2009JG001221.

NOAA (2021a) Record-breaking Atlantic hurricane season draws to an end | National Oceanic and Atmospheric Administration. ⟨https://www.noaa.gov/media-release/record-breaking-atlantic-hurricane-season-draws-to-end⟩. Accessed 7 Nov 2021.

NOAA (2021b) Hurricane Costs. ⟨https://coast.noaa.gov/states/fast-facts/hurricane-costs.html⟩.

Nwakuya, M.T., Nwakuya, M.T., Nwabueze, J.C., 2018. Application of Box-Cox transformation as a corrective measure to heteroscedasticity using an economic data. Am. J. Math. Stat. 8, 8–12. https://doi.org/10.5923/j.ajms.20180801.02.

O'Connell, B.M., Conkling, et al (2016) FIA Database Description and User Guide for Phase 2 (version: 6.1) The Forest Inventory and Analysis Database: Database Description and User Guide for Phase 2 (version 6.1).

Ojha, S.K., Naka, K., Dimov, L.D., 2020. Assessment of disturbances across forest inventory plots in the southeastern United States for the period 1995-2018. Sci 66, 242–255. https://doi.org/10.1093/forsci/fxz072.

Oswalt S., Miles P.D., Pugh S. a., Smith W.B. (2018) Forest Resources of the United States, 2017: a technical document supporting the Forest Service 2020 update of the RPA Assessment. Washington DC.

Pati, P.K., Kaushik, P., Khan, M.L., Khare, P.K., 2022. Allometric equations for biomass and carbon stock estimation of small diameter woody species from tropical dry deciduous forests: support to REDD+. Trees People 9, 100289. https://doi.org/10.1016/j.tfp.2022.100289.

Paul McLean, J., Zhang, T., Bardet, S., et al., 2011. The decreasing radial wood stiffness pattern of some tropical trees growing in the primary forest is reversed and increases when they are grown in a plantation. Ann. Sci. 68, 681–688. https://doi.org/10.1007/s13595-011-0085-z.

Peltola, H., Kellomäki, S., Väisänen, H., Ikonen, V.P., 1999. A mechanistic model for assessing the risk of wind and snow damage to single trees and stands of Scots pine, Norway spruce, and birch. Can. J. Res. 29, 647–661. https://doi.org/10.1139/x99-029.

Peneva-Reed, E.I., Krauss, K.W., Bullock, E.L., et al., 2021. Carbon stock losses and recovery observed for a mangrove ecosystem following a major hurricane in Southwest Florida. Estuar. Coast Shelf Sci. 248, 106750 https://doi.org/10.1016/j.ecss.2020.106750.

Petersson, H, Holm, S, Ståhl, G, et al., 2012. Individual tree biomass equations or biomass expansion factors for assessment of carbon stock changes in living biomass - A comparative study. For Ecol Manage 270, 78–84. https://doi.org/10.1016/j.foreco.2012.01.004.

Platt, W.J., Doren, R.F., Armentano, T.V., 2000. Effects of Hurricane Andrew on stands of slash pine (Pinus elliottii var. densa) in the everglades region of south Florida (USA). Plant Ecol. 146, 43–60. https://doi.org/10.1023/A:1009829319862.

Pohjankukka, J., Pahikkala, T., Nevalainen, P., Heikkonen, J., 2017. Estimating the prediction performance of spatial models via spatial k-fold cross validation. Int J. Geogr. Inf. Sci. 31, 2001–2019. https://doi.org/10.1080/13658816.2017.1346255.

Pugh, Scott A., Turner, et al (2018) FIA Database Population Estimation User Guide for Phase 2 The Forest Inventory and Analysis Database: Population Estimation User Guide.

R Core Team (2021) Report and Cite Packages. ⟨https://cran.r-project.org/web/packages/report/vignettes/cite_packages.html⟩. Accessed 24 Apr 2024.

Rivera-Monroy, V.H., Danielson, T.M., Castañeda-Moya, E., et al., 2019. Long-term demography and stem productivity of Everglades mangrove forests (Florida, USA): resistance to hurricane disturbance. Ecol. Manag. 440, 79–91. https://doi.org/10.1016/j.foreco.2019.02.036.

Rodríguez, J.D., Pérez, A., Lozano, J.A., 2010. Sensitivity analysis of k-fold cross validation in prediction error estimation. IEEE Trans. Pattern Anal. Mach. Intell. 32, 569–575. https://doi.org/10.1109/TPAMI.2009.187.

Ryan, M.G., Binkley, D., Fownes, J.H., 1997. Age-related decline in forest productivity: pattern and process. Adv. Ecol. Res 27 213–262. https://doi.org/10.1016/s0065-2504(08)60009-4.

Schmidt, M., Hanewinkel, M., Kändler, G., et al., 2010. An inventory-based approach for modeling singletree storm damage - experiences with the winter storm of 1999 in southwestern Germany. Can. J. Res 40, 1636–1652. https://doi.org/10.1139/X10-099.

Sharma, A., Bohn, K.K., Nowak, J., Dwivedi, P., 2018. Economic feasibility of and vegetation responses to biomass harvest in managed loblolly pine plantations. J. Sustain 37, 445–458. https://doi.org/10.1080/10549811.2017.1417137.

Sharma, A., Ojha, S.K., Dimov, L.D., et al., 2021. Long-term effects of catastrophic wind on southern US coastal forests: lessons from a major hurricane. PLoS One 16, e0243362. https://doi.org/10.1371/journal.pone.0243362.

Smunt, T.L., 1999. Log-linear and non-log-linear learning curve models for production research and cost estimation. Int J. Prod. Res 37, 3901–3911. https://doi.org/10.1080/002075499189826.

Steel RGD, Torrie J.H. (1961) Principles and Procedures of Statistics with Special Reference to the Biological Sciences.

Stewart S.R. (2011) Tropic cyclone report Hurricane Ivan. Miami, Florida.

Sweet, W.V., Hamlington, B.D., Kopp, R.E., et al., 2022. Global and Regional Sea Level Rise Scenarios for the United States. NOAA Tech. Rep. NOS 01, 111.

Talkkari, A., Peltola, H., Kellomäki, S., Strandman, H., 2000. Integration of component models from the tree, stand and regional levels to assess the risk of wind damage at forest margins. Ecol. Manag. 135, 303–313. https://doi.org/10.1016/S0378-1127(00)00288-7.

Taylor B., Kirschenfeld C., Turpin R.K., Handley L.R. (2002) Seagrass Status and Trends in the Northern Gulf of Mexico: 1940–2002. Escambia, Florida.

U.S. Global Change Research Program, 2018. Climate science special report. US Glob. Chang Res Progr 1, 1–470. https://doi.org/10.7930/J0J964J6.

US EPA (2022) Climate Change Indicators: Weather and Climate. ⟨https://www.epa.gov/climate-indicators/weather-climate⟩. Accessed 9 Jun 2023.

USDA (2003) Forest Service Handbook. Washington DC.

USDA (2021) Wood handbook: wood as an engineering materia. Madison, Wisconsin.

Valinger, E., Fridman, J., 2011. Factors affecting the probability of windthrow at stand level as a result of Gudrun winter storm in southern Sweden. Ecol. Manag. 262, 398–403. https://doi.org/10.1016/j.foreco.2011.04.004.

Vecchi, G.A., Swanson, K.L., Soden, B.J., 2008. Climate change: whither hurricane activity? Science 80 (322), 687–689. https://doi.org/10.1126/science.1164396.

Vorster, A.G., Evangelista, P.H., Stovall, A.E.L., Ex, S., 2020. Variability and uncertainty in forest biomass estimates from the tree to landscape scale: the role of allometric equations. Carbon Balance Manag 15 (1), 20. https://doi.org/10.1186/s13021-020-00143-6.

Wong, T.T., Yang, N.Y., 2017. Dependency analysis of accuracy estimates in k-fold cross validation. IEEE Trans. Knowl. Data Eng. 29, 2417–2427. https://doi.org/10.1109/TKDE.2017.2740926.

Xi, W., Peet, R.K., Urban, D.L., 2008b. Changes in forest structure, species diversity and spatial pattern following hurricane disturbance in a Piedmont North Carolina forest, USA. J. Plant Ecol. 1, 43–57. https://doi.org/10.1093/jpe/rtm003.

Xi, W., Peet, R.K., Decoster, J.K., Urban, D.L., 2008a. Tree damage risk factors associated with large, infrequent wind disturbances of Carolina forests. Forestry 81, 317–334. https://doi.org/10.1093/forestry/cpn020.

Zampieri, N.E., Pau, S., Okamoto, D.K., 2020. The impact of Hurricane Michael on longleaf pine habitats in Florida. Sci. Rep. 10 (1), 11. https://doi.org/10.1038/s41598-020-65436-9.

Zeileis, A., 2004. Econometric computing with HC and HAC covariance matrix estimators. J. Stat. Softw. 11, 1–17. https://doi.org/10.18637/JSS.V011.I10.

Zeileis, A., Köll, S., Graham, N., 2020. Various versatile variances: an object-oriented implementation of clustered covariances in r. J. Stat. Softw. 95 (1), 36. https://doi.org/10.18637/JSS.V095.I01.

Zeng, H., Chambers, J.Q., Negrón-Juárez, R.I., et al., 2009. Impacts of tropical cyclones on U.S. forest tree mortality and carbon flux from 1851 to 2000. Proc. Natl. Acad. Sci. USA 106, 7888–7892. https://doi.org/10.1073/pnas.0808914106.

Zhang, W., Vecchi, G.A., Murakami, H., et al., 2016. 26. Influences of natural variability and anthropogenic forcing on the extreme 2015 accumulated cyclone energy in the Western North Pacific. Bull. Am. Meteor. Soc. 97 https://doi.org/10.1175/BAMS-D-16-0146.1.